Journal of Electroanalytical Chemistry 812 (2018) 28–36

Contents lists available at ScienceDirect

Journal of Electroanalytical Chemistry

journal homepage: www.elsevier.com/locate/jelechem

Tubular-structured polypyrrole electrodes decorated with gold nanoparticles for electrochemical sensing

E. Gutiérrez Pineda[a,b], M.J. Rodríguez Presa[a], C.A. Gervasi[a,b], A.E. Bolzán[a,*]

[a] Instituto de Investigaciones Fisicoquímicas Teóricas y Aplicadas (INIFTA), Universidad Nacional de La Plata — CONICET, Sucursal 4 Casilla de Correo 16, (1900) La Plata, Argentina

[b] Area Electroquímica, Dept. Ing. Química, Facultad de Ingeniería, Universidad Nacional de La Plata, La Plata (1900), Argentina

ARTICLE INFO

Keywords:
Gold nanoparticles
Polypyrrole
Electrodeposition
Hydroxylamine
Nitrite
Sensors

ABSTRACT

The electrosynthesis and characterisation of polypyrrole(PPy) films with a micro-tubular structure decorated with gold nanoparticles is described. The PPy films were characterised by means of voltammetric and electrochemical impedance spectroscopy measurements. The tubular structure of the PPy films were obtained under potentiostatic conditions in freshly prepared sodium salicylate solutions. Voltammetric response of the PPy films shows that its behavior turns more reversible as the electropolymerization charge of the film increases. SEM images show the appearance of the tubular structure for an electrodeposition time higher than 2 min. The tubular-structured PPy film showed an rms of ca. 600 nm as determined from AFM imaging. These PPy films were subsequently decorated with gold nanoparticles obtained by a double step potentiostatic electrodeposition routine that allowed fine control of deposit characteristics. Analysis of deposits was performed by means of SEM and AFM nanoscopy. Statistical analysis of particles size distribution show that the maximum value appeared for 60 nm, but a significant amount of particles between 100–200 nm were also observed. The sensing capability of these composite electrodes was tested for the determination of hydroxylamine, nitrite and their mixture in solutions of different pH. Results showed a successful route of synthesis of a nanocomposite electrode with promising applications in electrochemical sensing.

1. Introduction

Electrochemical sensing requires the development of electrodes composed by materials with high electrocatalytic activity and at the same time a high exposed specific area. Due to their electrocatalytic properties, noble metals have usually been the first choice in electroanalytical applications. During recent years, the use of noble metal nanoparticles has been particularly emphasised and the incorporation of nanoparticles into different matrices to form the so-called nanocomposite films have attracted much attention for the development of electrochemical sensors [1]. For instance, fabrication of gold nanoparticles is a common procedure nowadays that has been used to produce, for example, gold dispersed carbon-paste electrodes, self-assembled monolayers, deposits on conducting and non-conducting polymers. In the case of polymers as substrates, it has been shown that most of the desirable properties of polymer/metal nanoparticles composites depend on metal nanoparticle dispersion and surface properties [2].

Electropolymerisation provides a simple and rapid method of controlling the thickness of a conductive polymer film adhered to the surface of an electrode of any size and shape. Probably one of the most representative and used conductive polymer is polypyrrole (PPy), which can be prepared either chemically or electrochemically. It has been widely used in electroanalytical applications, such as immunosensors [3], enzyme biosensors [4], DNA sensors [5], among others. More recently, imprinted polypyrrole membranes have been used for sensing dapsone [6]. The interest in PPy resides in the fact that it is a polymer that exhibits reasonably high conductivity in the oxidised state, good chemical stability and can be prepared in aqueous solutions [7], making it one of the most versatile conductive polymers in electrochemistry [8]. As a consequence, it has not only been used in the development of sensors [9,10], but also in corrosion protection [11–13] and the development of batteries [14,15] and supercapacitors [16,17]. In the case of sensors, PPy films may offer a suitable matrix for the deposition of the electrocatalytic material, resulting in a composite material that exhibits a low ohmic-drop pathway to the arrays of deposited micro- or nanoparticles of a sensing material. The use of highly dispersed gold nanoparticles are of particular interest due to their outstanding electrocatalytic and optical properties that, in addition to good biocompatibility, make them an attractive material for

* Corresponding author.
E-mail address: aebolzan@inifta.unlp.edu.ar (A.E. Bolzán).

https://doi.org/10.1016/j.jelechem.2018.01.047
Received 9 August 2017; Received in revised form 6 November 2017; Accepted 24 January 2018
Available online 31 January 2018
1572-6657/

designing electrochemical sensors and biosensors [18,19]. Contrary to simple flat smooth gold electrodes, Au nano- and microstructures on PPy provide large active surface area films whose thickness and morphology depend on the formation conditions of both, the PPy film and the gold deposit [20].

It is well known that the physical and spectroscopic properties of a PPy film depend strongly on the nature of the solvent, the supporting electrolyte, the solution pH, the monomer concentration, and eventually on the electrodeposition routine. The electrodeposition routine can be either a simple potentiostatic step, a repetitive voltammetric scan, a galvanostatic procedure, and in some cases it can be also run in the presence of gold ions in order to build up at the same time the PPy film with the formation of the gold deposit [10,21]. On the other hand, by changing the supporting electrolyte different PPy film morphologies can be obtained such as spherical particles in potassium tetraoxalate [22], large porous structures in dodecyl sulphate[9], nanowires in lithium perchlorate [23] and hollow microtubes of rectangular cross-section in salicylate solutions [24].

Different proposals have also been reported for producing an electroactive film of gold, particularly at the nanosize level, such as embedding in three-dimensional sol-gel networks [25], electrodepositing on choline films formed on glassy carbon electrodes [26] or on ultrathin overoxidised PPy films on glassy carbon [9], co-depositing under galvanostatic conditions to form a nanocomposite with PPy on glassy carbon [27], and depositing on PPy nanowires [23] or on graphite pencil electrodes [28], among other examples. Furthermore, the electrodeposition process can be performed by using galvanostatic [2,27,29], potentiostatic [22] or potential cycling [18,23,26,30] techniques or by simple immersion of electrodes in a gold ions-containing solution [28,31].

In a previous work, we reported the electrochemical synthesis of composite electrodes consisting of PPy films deposited on stainless steel substrates, decorated with gold nanoparticles and showed their electrocatalytic properties towards the electro-oxidation of hydrazine and hydroxylamine [20]. We reported the formation of either worm-like or columnar PPy structures depending on the nature of the electropolymerisation electrolyte. The present work is related to the electrosynthesis of PPy films with tubular structure in sodium salicylate solutions and their subsequent decoration with gold nanoparticles under potential controlled conditions to obtain a composite electrode suitable for electrochemical sensing. The composite electrodes were prepared on comparatively low-cost stainless steel discs, which provide a stable material as substrate as posible corrosion processes are already inhibited by the protective PPy film [11,32]. Surface morphology was studied by scanning electron microscopy and atomic force (SEM) and atomic force nanoscopy (AFM). The electrochemical properties of the films were studied by cyclic voltammetry and electrochemical impedance spectroscopy (EIS) and the suitability as electrochemical sensor tested in different analytes containing hydroxylamine and nitrite, molecules whose detection and quantitative determination in aqueous solutions are relevant to the chemical, pharmaceutical, agricultural and food industries [33]. Particularly, it is interesting to examine the possibility of simultaneous detection and determination of mixtures and the use of the sensor in a wide range of pH compatible with the stability of the chemicals to be determined, conditions that fulfill the present composite electrode.

2. Experimental method

2.1. Reagents

Pyrrole (Sigma-Aldrich) was purified by distillation under reduced pressure before use. $HCl_4Au \cdot 3\ H_2O$ (Aldrich, p.a.) was used for the electrodeposition of gold on the PPy films. Testing analytes were prepared using hydroxylamine, NH_2OH (Fluka, p.a.) and sodium nitrite ($NaNO_2$; Merck p.a.). All solutions were prepared with Milli-Q water.

2.2. Electrode preparation

The substrate electrodes consisted of discs (0.12 cm^2 area) of stainless steel (SS) grade AISI 304 (UNS S30400). They were mechanically polished with alumina (0.3 μ m) suspension and after deposition, the PPy films were washed with ethanol (96% v/v Sigma-Aldrich) and Milli-Q water to remove the rests of the salicylate salt and obtain a clean starting surface. A conventional three-electrode cell was used for the formation of the PPy layer on the SS substrate. The electropolymerisation process was performed at constant potential (E = 0.80 V vs SCE) in aqueous 0.25 M pyrrole + 0.5 M $C_7H_5NaO_3$. Polymerisation time was changed between 30 s and 5 min in order to analyse changes in both film morphology and electrochemical response, as a function of polymer thickness. It should be pointed out that the electropolymerisation was performed with readily fresh distilled pyrrole in order to obtain the tubular structure of the polymeric film. If pyrrole was used after only few hours of distillation, although being kept refrigerated in the absence of light and under nitrogen atmosphere, the resulting polymer film did not exhibit tubular structure but the columnar structures already reported [20].

The Au electrodeposition on the PPy/SS electrodes was performed using a 0.001 M $HAuCl_4$ + 0.005 M H_2SO_4 solution by applying a double step potentiostatic routine. Thus, the working electrode was initially set at 0.8 V during 10 s to activate/clean the electrode. Afterwards, the potential was stepped to − 0.8 V during 0.1 –0.5 s, to allow the formation of Au nuclei on the PPy surface, and eventually stepped to 0.1 V during 0.5 –60 s to grow the Au nuclei previously formed.

2.3. Instruments and experimental techniques

Voltammetry and chronoamperometry measurements were made by using a PGSTAT 204 (Metrohm Autolab B.V.) potentiostat. Electrochemical impedance spectroscopy measurements were carried out by using a Zahner IM6d electrochemical workstation by applying an AC signal of 0.01 V amplitude and sweeping the frequency f from $10^{-3} \leq f$ to 60×10^3 Hz. Electroanalytical experiments were run by means of differential pulse voltammetry (DPV), by employing a pulse height of 0.005 V with amplitude of 0.05 V, and pulse time of 200 ms.

Electrochemical experiments were made at room temperature under nitrogen atmosphere. Potentials are referred to the saturated calomel electrode (SCE) scale.

The morphological characterisation of PPy and Au/PPy deposits was made by using an environmental scanning electron microscope (FEI Quanta 200 ESEM, accelerating voltage 12–15 kV, Everhardt-Thornley detector) equipped with and Oxford Inca 300 EDX system for chemical analysis.

3. Results and discussion

3.1. Electroformation of PPy tubes and their electrochemical response

As it is well-known from the literature, properties and morphology of electrochemically formed PPy films can be very different depending on the preparation conditions. Therefore, the first aspect to analyse when employing PPy films as part of composite electrodes, is to establish both, the morphological characteristics of the films and their electrochemical response. At variance with data reported in a previous work [20], the formation of PPy tubes in $C_7H_5NaO_3$ was accomplished by starting the electropolymerisation process immediately after the monomer distillation. Under this condition, i.e. when very freshly distilled pyrrole was employed, the formation of a PPy film exhibiting a structure of micro-tubes was achieved. To follow the appearance of the tubular structure, the electropolymerisation process on the SS substrates was performed applying a constant potential of 0.8 V during different times. Thus, when the PPy films were grown during less than

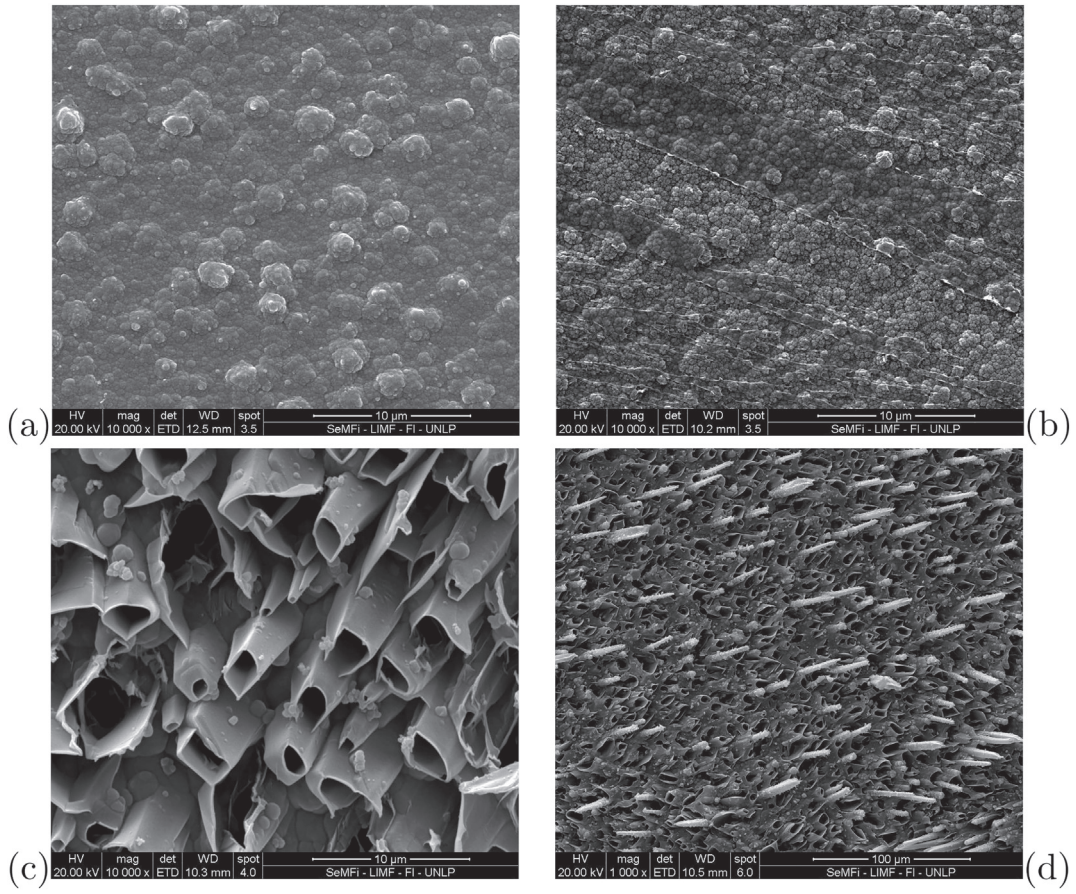

Fig. 1. SEM images of PPy films formed at 0.8 V in 0.1 M $C_7H_5NaO_3$ during: 1 min (a), 2 min (b), 3 min (c) and 5 min (d).

3 min the SS surface resulted covered by a cauliflower-type PPy film (Fig. 1a, b). On the other hand, when the polymerisation time was raised to 3 min, the morphology of the film showed a tubular structure (Fig. 1c). However, if the electropolymerisation time was further increased, the tubes start to close steadily due to the progressive aggregation of polymeric material to the external walls (a feature incipiently observed for $t = 3$ min) and at the open side of the tubes (Fig. 1d).

The electrochemical response of the PPy films obtained at different polymerisation times was first studied by running cyclic voltammograms at 0.050 V s^{-1} between − 1.0 and 0.8 V, i.e. the potential range corresponding to the polymer redox couple. Thus, when the PPy film exhibits a cauliflower-like structure, the voltammogram shows an anodic current peak at ca. 0.05 V and a small cathodic peak at ca. − 0.8 V that is preceded by a small hump at ca. − 0.5 V (Fig. 2). As the electropolymerisation time is increased, and the tubular structure is formed, the voltammetric response shows well-defined anodic and cathodic current peaks at ca. 0.28 V and − 0.45 V, respectively. Seemingly, the tubular structure exhibits a better separation between faradaic and capacitive contributions of the polymeric deposited film.

The electrochemical characterisation of the conductive polymer films was also performed by means of EIS measurements, a well established technique for examining the properties of surface-modified electrodes, which has been widely used for characterising electrochemical processes occurring in conductive polymer films [2,29,30,34]. The "ideal" impedance response of an electroactive polymer film is usually described as a separate Randles circuit behavior at high frequencies with a Warburg section at intermediate frequencies, and a purely capacitive behavior, due to the redox capacitance, in the low frequency range.

To characterise the tubular-structured PPy films, comparative EIS

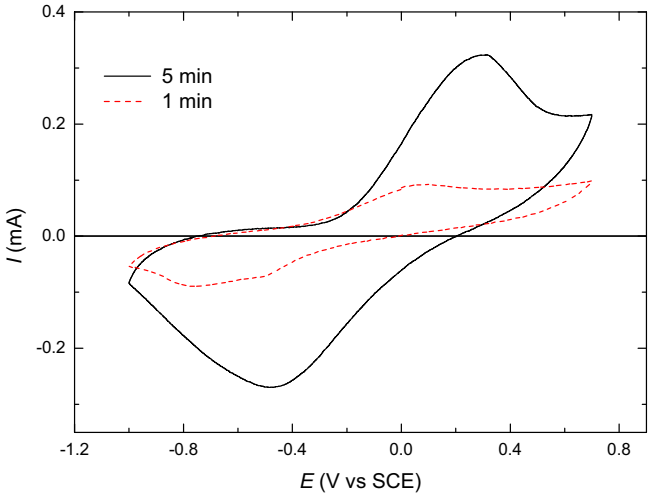

Fig. 2. Cyclic voltammograms run in $NaC_7H_5O_3$ 0.5 M corresponding to stainless steel electrodes covered by a cauliflower-like (1 min) and tubular-structured (5 min) PPy films.

measurements were made for both, the thin cauliflower-type and the thicker tubular-structured PPy films, at the open circuit potential (OCP), i.e. equilibrium conditions, and at OCP ± 0.20 V, i.e. a potential value at which PPy films are in the oxidation state and, consequently, exhibit good electrical conduction. At first glance, the resulting Nyquist plots show a marked difference between both types of polymer structures (Fig. 3). First of all, the impedance values are significantly smaller in the case of the tubular films indicating a larger electrochemical active area, although always a single time constant at high frequencies is observed. This time constant is related to the charge

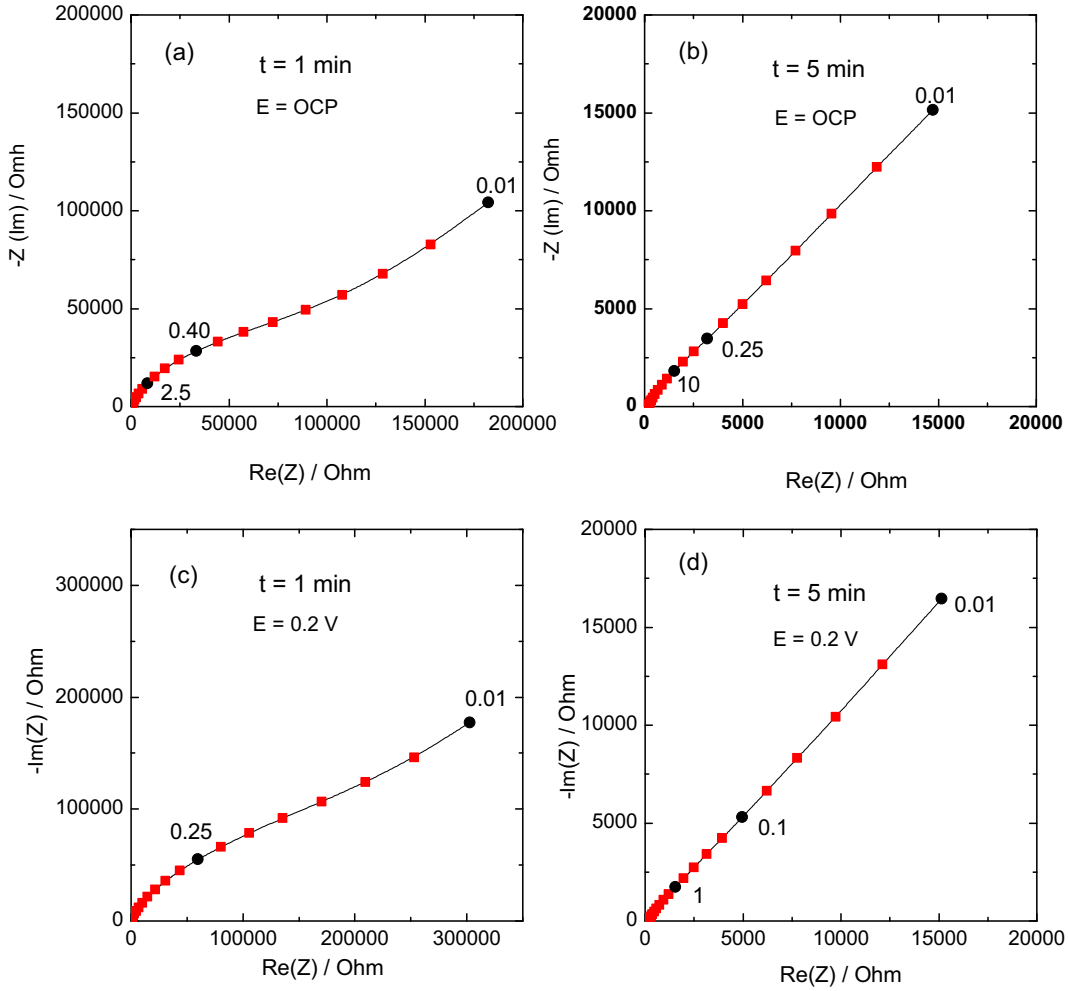

Fig. 3. Nyquist plots measured in 0.1 M $C_7H_5NaO_3$ at the OCP (a, c) and at 0.2 V (b, d) for PPy films grown during 1 min (a, c) and 5 min (b, d). Frequencies are indicated in Hz.

transfer process corresponding to the charge/discharge of the PPy matrix. As the AC signal frequency is decreased, the response of the thin films with a cauliflower-type PPy structure (Fig. 3a, c) show a low tilt angle without approaching the vertical linear behavior expected for a pure capacitive response. In general, this tilt angle is expected to decreases as the spread factor, which measures how inhomogeneous the film is due to variations in morphology from one region to another, increases [35].

In the case of the PPy films with tubular structure (Fig. 3b, d), the Nyquist plot exhibits a Warburg contribution from about 1 Hz downwards, without any evidence of tendency to a capacitive response at intermediate frequency values.

3.2. Electrodeposition of Au

As mentioned above, the tubular structure appears after 2 min of anodic polarisation of the SS electrodes in the pyrrole containing $C_7H_5NaO_3$ solution, and, as the anodisation time was increased, the continuous electrodeposition of PPy resulted in the obstruction of open tubes, so that, for the decoration process with gold nano-particles, the anodisation time was set to 3 min (0.38 C cm^{-2} electrodeposition charge). The electrodeposition of gold atoms on the PPy tubular matrix was performed in two steps, i.e. in the first one, the electrode was set at a sufficiently negative potential for a short time to produce the instantaneous activation of the surface sites on the PPy electrode and then the potential was set at a potential value where the growth of the initial nuclei could proceed. The amount of gold was then determined by the time elapsed at this potential. Accordingly, the potential was stepped first to − 0.8 V during 0.5 s and then stepped to 0.1 V during 0.5–60 s. Thus, the SEM micrographs corresponding, for instance, to gold deposit grown during 30 s (Fig. 4) show the presence of randomly distributed particles. The size distribution determined for these conditions shows that the size of most of the particles are around 25–75 nm average size.

3.3. Electrochemical behaviour of the composite electrodes as sensors

As reported in a previous work [20], the electrodeposition of nano- and micro-particles on PPy films, results in an enhancement of the electrocatalytic properties of the composite electrode, as compared to plain smooth gold electrodes. The advantage of supporting the gold particles onto the PPy matrix is not only the higher electrocatalytic activity, expressed through the decrease in the potential threshold for electro-oxidation of organic molecules, but also the increase in the active surface thanks to the 3D structure of the PPy film. The tubular structure of the PPy matrix would act as a brush with open hairs, a fact that increases the contact with the analyte to be sensed. As shown above, the electrocatalytic gold particles are deposited not only on the external surface of the tubes, but also inside them, a fact that should increase the sensitivity of the electrodes as compared to those supporting PPy solid structures, such as worm-like or columnar ones [20]. In order to confirm that these PPy tubular electrodes covered by Au nanoparticles exhibit good electrocatalytic properties for the case of the analytes of interest in this work, comparative voltammograms were run for the electro-oxidation of hydroxylamine and nitrite ions on a smooth

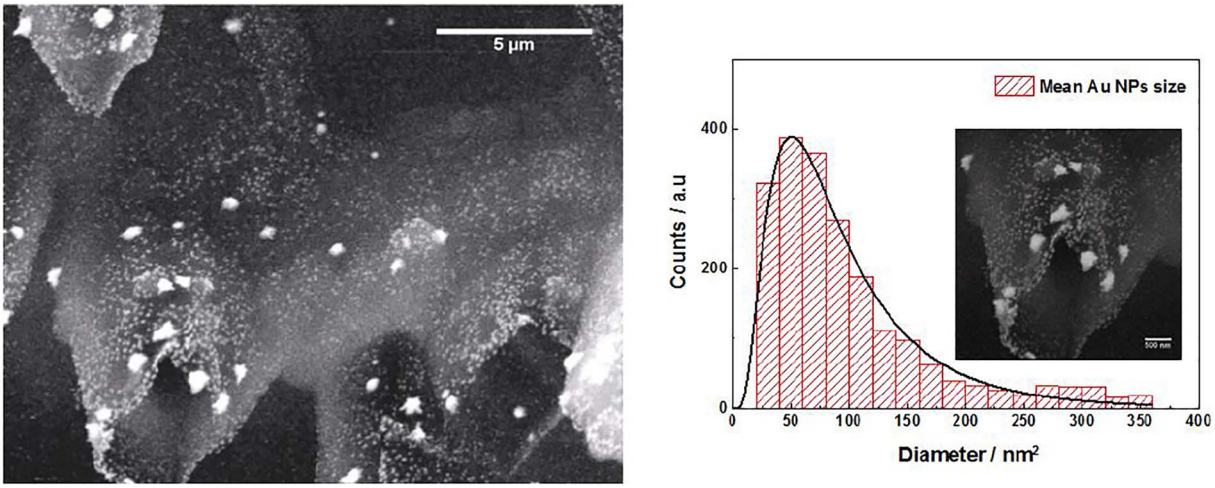

Fig. 4. SEM images of the gold deposit on the tubular-structured PPy film and the corresponding size distribution of Au Nps. PPpy film formed at 0.8 V during 3 min in 0.1 M $C_7H_5NaO_3$. Au nuclei were formed at − 0.8 V during 0.5 s and grown at 0.1 V during 30 s.

gold electrode, on a stainless steel electrode covered by the PPy deposit and finally on a gold-decorated tubular-structured PPy electrode. Accordingly, voltammetric results obtained in 0.1 M PBS at pH 7.0 show that, as expected, the plain PPy electrode shows no particular activity for the electro-oxidation reaction of either hydroxylamine or nitrite ions, while the Au-decorated PPy electrodes exhibit the corresponding electro-oxidation current peaks at potentials less positive than in the case of a smooth gold electrode (Fig. 5 a, b). In the case of hydroxylamine, the electro-oxidation peak appears at ca. 0.15 V less positive value whereas for the case of nitrite ions, the potential difference is slightly higher, i.e. ca. 0.2 V. The increase in the electrocatalytic activity of the composite electrode, as compared to the smooth gold electrode, indicates that the gold decoration of the PPy matrix film deposited on a SS substrate generates not only an open 3D electrode structure, but also a good electrocatalytic surface for sensing both hydroxylamine and nitrite ions in solutions. This is particularly interesting for the case of nitrite as the electro-oxidation reaction of nitrite on GC is known to be very sluggish [36].

As observed from the profiles obtained from the cyclic voltammograms, the underlying large capacitive contribution from the PPy layer makes it difficult to determine the actual peak currents corresponding to the electro-oxidation of the analytes. Therefore, differential pulse voltammetry was used for the electroanalytical determinations. This differential pulse technique has well-known advantages in electroanalysis, such as well-defined peak-shaped response and reduced capacitance effects [37]. For this reason, DPV is, along with the square wave voltammetry, the most employed voltammetric technique for electroanalytical determinations [23,36], although linear voltammetric sweeps were employed in several cases [22,25].

Furthermore, to test the capability of these electrodes as electrochemical sensors, three different situations were considered, namely the determination of hydroxylamine and nitrite ions alone, and a mixture of them in solution. For this purpose, the sensing electrode was prepared by growing the PPy film during 3 min in the salicylate solution, then

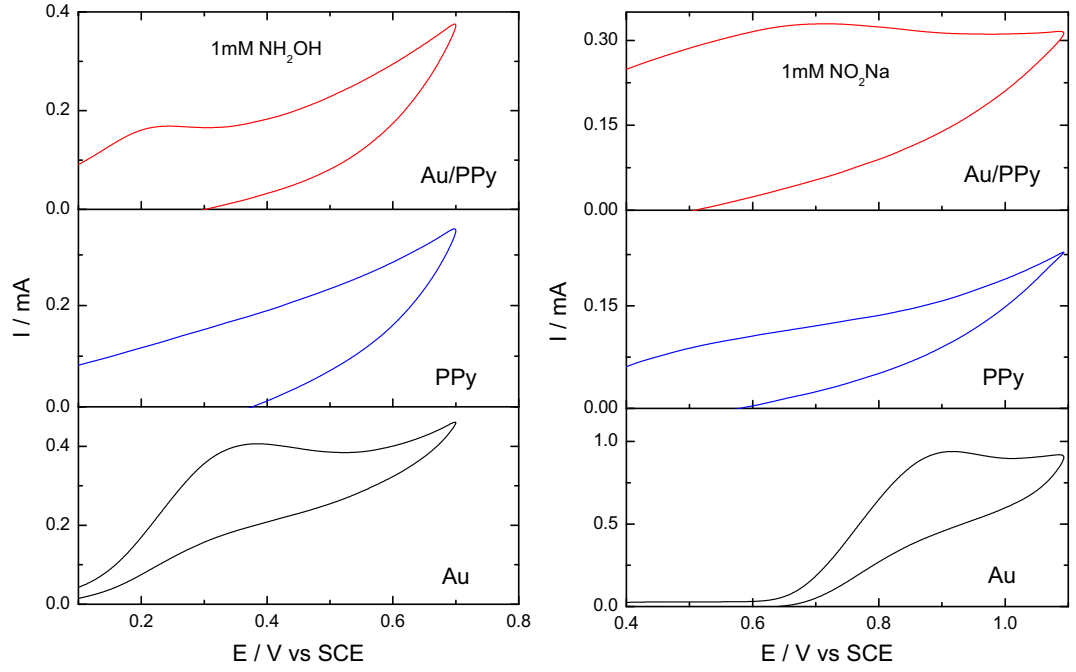

Fig. 5. Comparative voltammograms related to the electro-oxidation of NH_2OH (a) and NO_2^- (b) in 0.1 M PBS (pH = 7.0) on different electrodes as indicated. Analyte concentration: 1 mM; $\nu = 0.2\,V\,s^{-1}$.

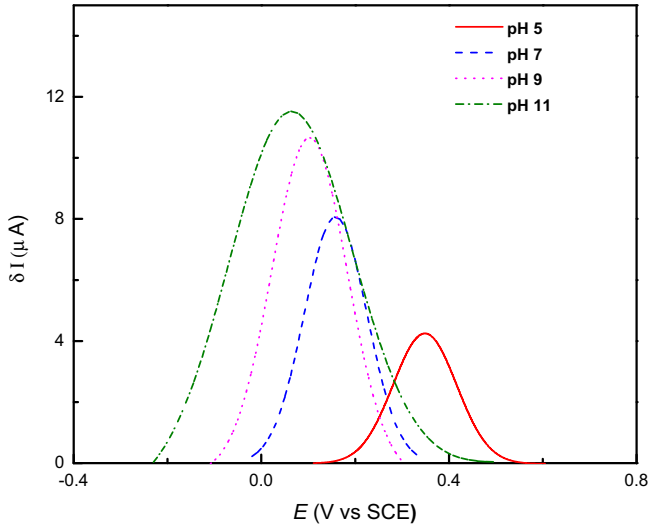

Fig. 6. DPV of 1 mM NH_2OH electro-oxidation in 0.1 M PBS at different pH values, as indicated.

transferred to the acid solution containing the gold salt, where they were decorated with gold particles by applying an electrodeposition routine consisting of setting the electrode at − 0.8 V during 0.5 s and step to 0.1 V for 30 s (Au charge = 0.015 C cm^{-2}).

The electroanalytical experiments were run in 0.1 M phosphate buffer solution (PBS) and, depending on the molecule to be sensed, the pH was adjusted by small additions of 0.1 M NaOH or 0.5 M H_2SO_4. The sensing electrodes were tested through differential pulse voltammetry (DPV) and square wave voltammetry (SWV) measurements, although for the sake of simplicity only the DPV data are presented here. Both DPV and SWV are the most adequate techniques for sensing purposes, as they, at variance with linear and cyclic sweep voltammetry, sample the current just before the potential is changed, decreasing the effects of charging currents. In the present case, DPV runs were performed using a 0.005 V pulse height, 0.05 V amplitude, and a period of 200 ms. Although the experiments were run using a 0.1 M PBS as base electrolyte, the pH value was adjusted during the experiments in order to obtain the highest current response for each analyte, as explained below.

3.3.1. Electrochemical determination of hydroxylamine

The relevance of the quantitative determination of hydroxylamine results from the fact that this molecule is considered as a key intermediate in the nitrogen cycles and the production of nitrous oxide. Furthermore, it is a common reducing agent widely used in industry and pharmacy in the synthesis of pharmaceutical intermediates and final drug substances, and, at the same time, it is also a well-known mutagen and moderately toxic substance, harmful for humans and plants, making the sensitive detection of the molecule of particular interest in the field of environmental and biological analysis [23,30]. The oxidation of hydroxylamine can be expressed through a global four-electron process that is pH-dependent according to [38]:

$$2NH_2OH \longrightarrow N_2O(g) + H_2O + 4H^+ + 4e^- \quad (1)$$

or

$$2NH_2OH + 4OH^- \longrightarrow N_2O(g) + 5H_2O + 4e^-. \quad (2)$$

Accordingly, DPV measurements were run at a constant concentration of 1 mM NH_2OH in a PBS solution at different pH values. The pH of the base electrolyte was adjusted by adding small aliquots of either H_2SO_4 or NaOH.

Hydroxylamine presents a nonprotonated form NH_2OH for pH above 5.9 and a protonated form NH_3OH^+ at pHs below 5.9, being the protonated form the less active. Accordingly, the DPV curves obtained for pH values between 5 and 11, show that the electro-oxidation current peak increases and moves negatively as the pH is increased from 5 to 11 (Fig. 6). Thus, the peak potential moves from 0.350 V at pH = 5 to 0.066 V at pH = 11, appearing the major potential shift when increasing the pH from 5 to 7, i.e when the hydroxylamine molecule changes from protonated to nonprotonated.

According to these results, the pH for the electroanalytical measurements was adjusted to 9. Thus, under this condition, the DPV curves show a current peak at ca. 0.15 V that increases as the NH_2OH concentration is increased from 0.5 to 60 μM (Fig. 7a). The calibration curve obtained by plotting the peak current (actually δI_p) versus the NH_2OH concentration show two linear segments, as usually found in the literature [23,30]. The first one exhibits a slope of 0.32 μA μM^{-1} (Fig. 7b, inset) and the second one a slope of 0.08 μA μM^{-1}(Fig. 7b), with a detection limit for hydroxylamine determined as 0.226 μ M according to the calibration curve. This value compares very well to those reported in the literature for different modified electrodes [23,39,40]. The decrease in the current sensitivity as the NH_2OH concentration is

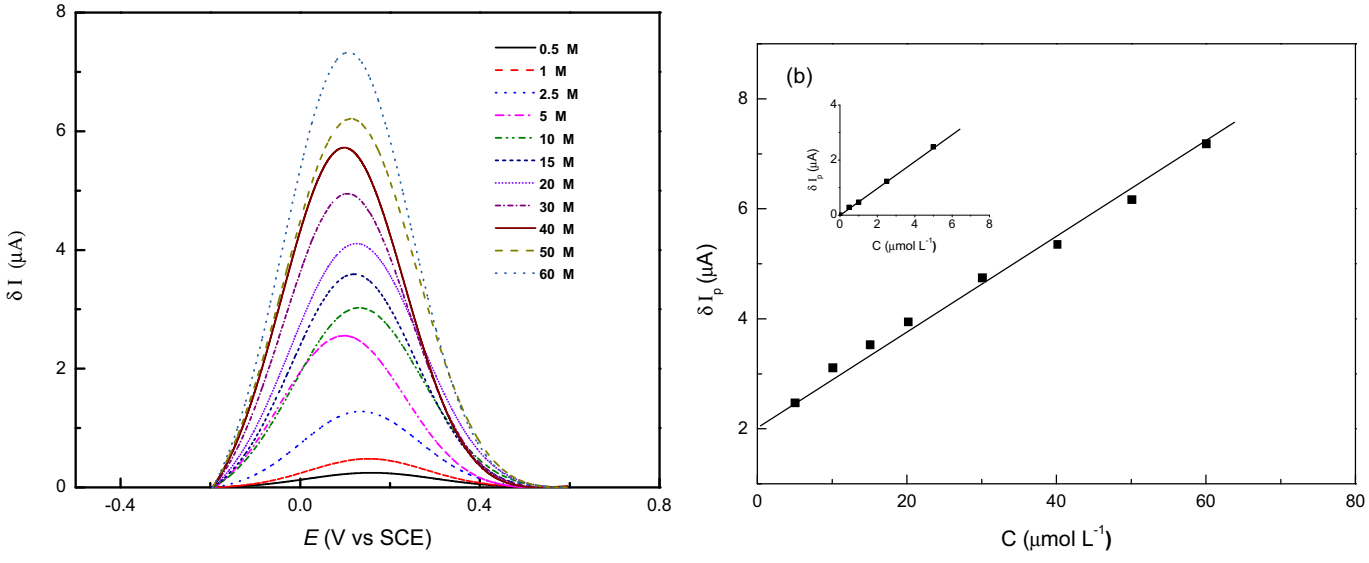

Fig. 7. (a) DPV at different hydroxylamine concentrations (as indicated) in 0.1 M PBS (pH = 9). (b) The calibration curve for hydroxylamine determination.

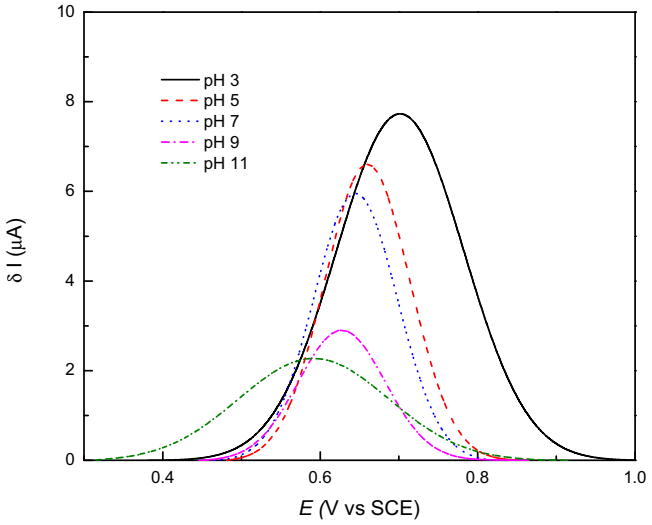

Fig. 8. DPV of 1 mM NO_2^- electro-oxidation in 0.1 M PBS adjusted at different solution pH values, as indicated.

increased, has been attributed to a decrease in the real electrocatalytic area of the electrode, i.e. the gold decorating particles. The decrease in area would be produced by the formation of bubbles of N_2O, as a main electro-oxidation product of NH_2OH, blocking the gold surface. As the NH_2OH concentration is increased, the amount of this product increases and consequently increases the size of the bubbles, which adhere to the catalytic sites and prevents new reacting molecules to arrive at the reaction interface. In fact, we have visually observed the presence of small bubbles when the concentration of hydroxylamine was sufficiently high.

3.3.2. Electrochemical determination of nitrite

The composite electrodes were also tested for nitrite determination. Nitrite is an important precursor in the formation of nitrosamines, many of which have been shown to be potent carcinogens in human bodies, and it has been amply used in the environment, beverages and food products as a preservative. On the other hand, nitrite can be present, along with other nitrogen-containing compounds, in a variety of industrial processes involving the participation of hydroxylamine or hydrazine [23]. Therefore, it results relevant the simultaneous detection of these compounds, particularly in the industries of chemical, pharmaceutical, food and agriculture products. For instance, the simultaneous electrochemical detection of hydrazine and nitrite has been proposed by using an electrochemical sensor consisting of gold nanoparticles embedded in a 3D sol-gel network employing a voltammetric routine [25]. In our case, we have then studied first the feasibility of using the electrodes in the detection of nitrite, and then in the mixture of nitrite and hydroxylamine.

As done before, DPV curves for the electro-oxidation of nitrite were first obtained for different pHs of the PBS solutions containing 0.001 M $NaNO_2$, to optimise the pH value for the detection of nitrite.

In this case, the DPV current peak moves from 0.7 to 0.58 V as the pH is increased from 3 to 11 and the peak current decreases strongly as the pH is increased (Fig. 8). This behaviour is consistent with previous data where it was shown that the peak current increased from pH 2 to 3.5, maintained from 3.5 to 4.5 and then rapidly decreased from pH 5 to 6 [41,42].

Accordingly, the solution pH was adjusted to 5 and DPV runs were made for nitrite concentrations increasing from 0.5 to 60 μ M. The DPV curves show a single current peak that steadily increases with nitrite concentration, with a peak potential centred at ca. 0.65 V (Fig. 9a). The DPV peak current versus nitrite concentration plot shows two well-defined linear regions. The first one appears between 0.5 and 6 μM and exhibits a slope of 0.29 μA μM^{-1}, while the second linear region appears for the concentration range from 10 to 60 μM with a slope of 0.05 μA μM^{-1}(Fig. 9b). The detection limit was determined as 0.61 μM. These results can be compared to those obtained for a nitrite sensor based on thionine modified aligned carbon nanotubes, where a linear response was observed between 50 and 500 μM with a detection limit of 1.12 μM [41], or to the sensor based on carbon paste electrode impregnated with a cobalt(II)-Schiff base complex, where the linear range was observed for 1 to 30 μM with a sensitivity of 3.05 μA μM^{-1} and a detection limit of 1.5×10^{-2} μM [42].

The two linear regions observed in the calibration plot can be in principle be assigned, similarly to the case of hydroxylamine, to the fact that the electrochemical oxidation of nitrite produces gaseous NO_2 as an intermediate species [36,43]

$$NO_2^- \longrightarrow NO_2(g) + e^- \quad (3)$$

$$2NO_2(g) + H_2O \longrightarrow NO_3^- + NO_2^- + 2H^+. \quad (4)$$

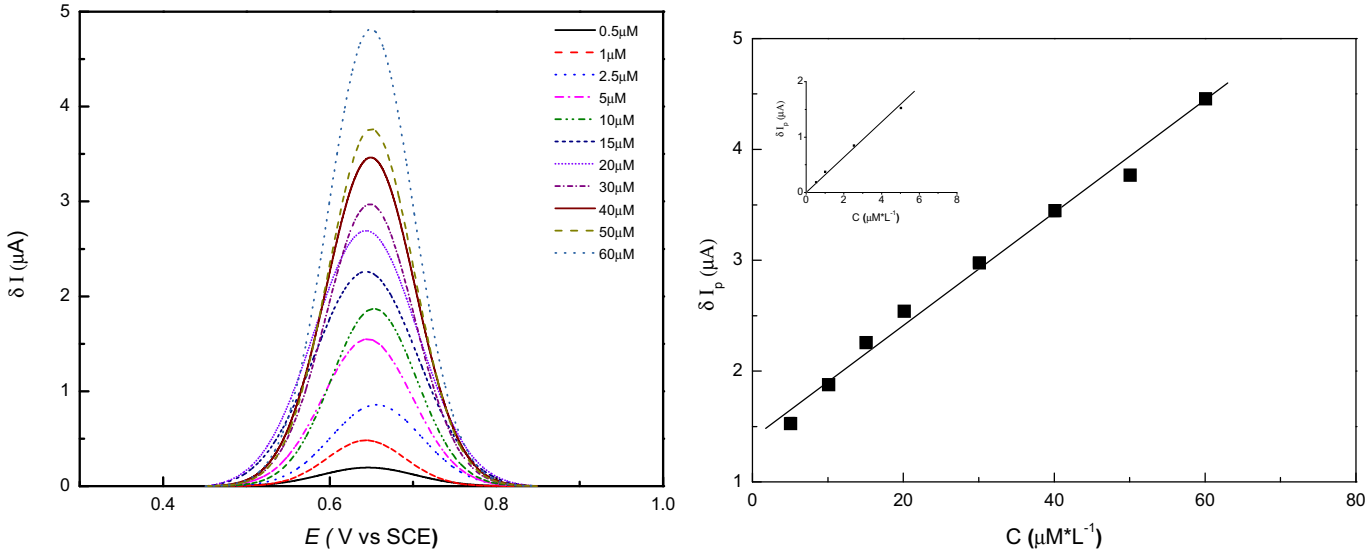

Fig. 9. (a) DPV at different nitrite ion concentrations (as indicated) in 0.1 M PBS (pH = 5). (b) Calibration curve for nitrite ion determination.

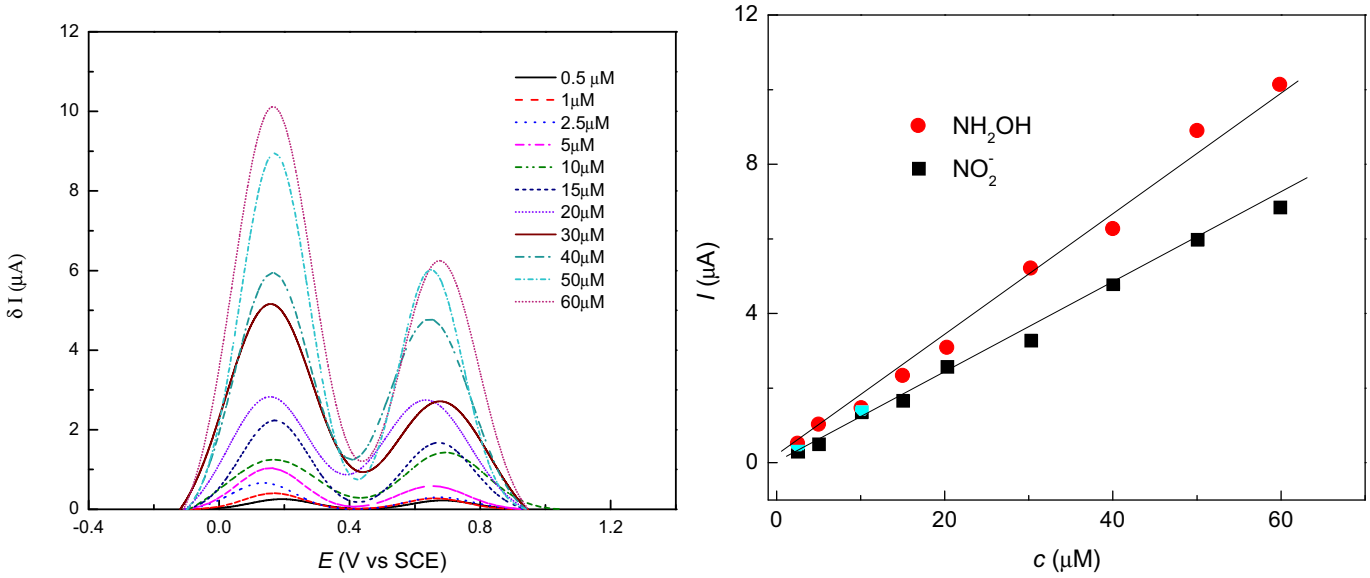

Fig. 10. (a) DPV at different equimolar hydroxylamine + nitrite concentrations (as indicated) in 0.1 M PBS (pH = 7). (b) The calibration curve for a solution containing equimolar concentrations of hydroxylamine and nitrite in 0.1 PBS at pH = 7.

3.3.3. Simultaneous electrochemical determination of hydroxylamine and nitrite

The sensing electrode was eventually used for the simultaneous electroanalytical determination of hydroxylamine and nitrite. For this purpose, the DPV measurements of the composite electrode in an analyte solution containing equimolar concentrations of both species were carried out. Preliminary runs were made to determine the solution pH value at which the concurrent determination would be more favourable. Therefore, DPV runs were made by varying the pH solution from 5 to 11, where two clear and well-separated current peaks were recorded, the first one corresponding to the electro-oxidation of hydroxylamine, and the second one, located at more positive potentials, is related to the electro-oxidation of nitrite, in good agreement with the results obtained for the separated compounds alone (Figs. 7 and 9).

The voltammograms showed that both current peaks moved to lower potentials as the solution pH was increased, and at the same time, the peak current ratio between hydroxylamine and nitrite tended to increase, i.e. the increase in pH favours the electro-oxidation of hydroxylamine with respect to nitrite. At the same time, the potential difference between both electro-oxidation processes increased from ca. 0.4 V at pH = 3 to ca. 0.5 V at pH = 9.

Therefore, considering the dependence of both reactions on pH, a value of 7 was selected for the concurrent determination of both species. For this purpose, solutions containing equimolar nitrite and hydroxylamine concentrations ranging from 0.5 to 60 μ M were studied. The resulting DPV data show the progressive increase in the corresponding current peaks located at ca. 0.15 V (hydroxylamine) and ca. 0.65 V (nitrite) as the analyte concentration is increased (Fig. 10). The corresponding calibration curve shows a linear response for the whole range measured with slopes of ca. 1.71×10^{-7}μ A μM^{-1} for hydroxylamine and ca. 1.16×10^{-7}μ A μM^{-1} for nitrite.

4. Conclusions

An effective strategy was implemented to develop gold nanoparticles/conducting polymer nanocomposites for electrochemical sensing. Under well-controlled electrochemical synthesis conditions, a PPy film exhibiting a tubular structure was obtained, which provided a well-exposed matrix structure for depositing gold particles at the micro- and nano-level sizes. A fine control of the amount and size of Au NPs is possible to be obtained by means of the double potential-step routine employed in this work. This provides an enhanced electrocatalytic behavior of these electrodes, as compared to that of Au surfaces. The use of these composite electrodes was successfully tested for the determination of hydroxylamine, nitrite and their mixture, two molecules of particular interest in the field of electrochemical sensing, and opens the possibility of using these electrodes for sensing other molecules that are electrocatalytically active on a gold surface.

Acknowledgements

This work was financially supported by the Agencia Nacional de Promoción Científica y Tecnológica of Argentina (ANPCYT PICT 2013-0387), the Consejo Nacional de Investigaciones Científicas y Técnicas (CONICET) and the Comisión de Investigaciones Científicas de la Provincia de Buenos Aires (CICPBA). AEB and CAG are members of CICPBA.

References

[1] C. Karuppiah, S. Palanisamy, S.M. Chen, S.K. Ramaraj, P. Periakaruppan, A novel and sensitive amperometric hydrazine sensor based on gold nanoparticles decorated graphite nanosheets modified screen printed carbon electrode, Electrochim. Acta 139 (2014) 157–164.
[2] X. Li, I. Zhitomirsky, Capacitive behaviour of polypyrrole films prepared on stainless steel substrates by electropolymerization, Mat. Lett. 76 (2012) 15–17.
[3] N. West, P. Baker, T. Waryo, F.R. Ngece, E.I. Iwuoha, C. O'Sullivan, I. Katakis, Highly sensitive gold-overoxidized polypyrrole nanocomposite immunosensor for antitransglutaminase antibody, J. Bioact. Compat. Polymers 28 (2013) 167–177.
[4] J. Njagi, S. Andreescu, Stable enzyme biosensors based on chemically synthesized Au-polypyrrole nanocomposites, Biosens. Bioelectron. 23 (2007) 168–175.
[5] E. Spain, T.E. Keyes, R.J. Forster, Polypyrrole-gold nanoparticle composites for highly sensitive DNA detection, Electrochim. Acta 109 (2013) 102–109.
[6] A. Afkhami, F. Gomar, T. Madrakian, Electrochemical sensor for dapsone using molecularly imprinted polypyrrole membrane as a recognition element, J. Electrochem. Soc. 162 (2015) B109–B113.
[7] R. Ansari Khalkhali, Electrochemical synthesis and characterization of electroactive conducting polypyrrole polymers, Russ. J. Electrochem. 41 (2005) 950–955.
[8] R. Ansari, Polypyrrole conducting electroactive polymers: synthesis and stability studies, E-J. Chem. 3 (2006) 186–201.
[9] J. Li, X.Q. Lin, Electrodeposition of gold nanoclusters on overoxidized polypyrrole film modified glassy carbon electrode and its application for the simultaneous determination of epinephrine and uric acid under coexistence of ascorbic acid, Anal. Chim. Acta 596 (2007) 222–230.
[10] A.M. Nowicka, M. Fau, T. Rapecki, M. Donten, Polypyrrole-au nanoparticles composite as suitable platform for DNA biosensor with electrochemical impedance spectroscopy detection, Electrochim. Acta 140 (2014) 65–71.
[11] M. González, S. Saidman, Electrodeposition of polypyrrole on 316L stainless steel for corrosion prevention, Corr. Sci. 53 (2011) 276–282.

[12] R. Ma, K. Sask, C. Shi, J. Brash, I. Zhitomirsky, Electrodeposition of polypyrrole-heparin and polypyrrole-hydroxyapatite films, Mater. Lett. 65 (2011) 681–684.
[13] D. Gopi, S. Ramya, D. Rajeswari, L. Kavitha, Corrosion protection performance of porous strontium hydroxyapatite coating on polypyrrole coated 316L stainless steel, Colloids Surf. B: Biointerfaces 107 (2013) 130–136.
[14] J. Wang, J. Chen, C. Wang, D. Zhou, C. Too, G. Wallace, Electrochemical synthesis of polypyrrole films using stainless steel mesh as substrate for battery application, Synth. Met. 153 (2005) 117–120.
[15] H.K. Song, G. Palmore, Redox-active polypyrrole: toward polymer-based batteries, Adv. Mat. 18 (2006) 1764–1768.
[16] X. Li, I. Zhitomirsky, Electrodeposition of polypyrrole-carbon nanotube composites for electrochemical supercapacitors, J. Power Sources 221 (2013) 49–56.
[17] P. Si, S. Ding, X.W.D. Lou, D.H. Kim, An electrochemically formed three-dimensional structure of polypyrrole/graphene nanoplatelets for high-performance supercapacitors, RSC Adv. 1 (2011) 1271.
[18] T. An, W. Choi, E. Lee, S.J. Cho, G. Lim, Fabrication of conducting polymer micro/nanostructures coated with Au nanoparticles for electrochemical sensors, J. Nanosci. Nanotechnol. 12 (2012) 4975–4978.
[19] S. Singh, D.V.S. Jain, M.L. Singla, One step electrochemical synthesis of gold-nanoparticles-polypyrrole composite for application in catechin electrochemical biosensor, Anal. Meth. 5 (2013) 1024.
[20] E. Gutiérrez Pineda, F. Alcaide, M.J. Rodríguez Presa, A.E. Bolzán, C.A. Gervasi, Electrochemical preparation and characterization of polypyrrole/stainless steel electrodes decorated with gold nanoparticles, ACS Appl. Mater. Interfaces 7 (2015) 2677–2687.
[21] T. Rapecki, M. Donten, Z. Stojek, Electrodeposition of polypyrrole-Au nanoparticles composite from one solution containing gold salt and monomer, Electrochem. Commun. 12 (2010) 624–627.
[22] D. Oukil, L. Benhaddad, L. Makhloufi, R. Aitout, B. Saidani, Gold nanoparticles modified polypyrrole/iron electrode used as sensor for hydrazine detection, Sens. Lett. 11 (2013) 395–404.
[23] J. Li, X. Lin, Electrocatalytic oxidation of hydrazine and hydroxylamine at gold nanoparticle–polypyrrole nanowire modified glassy carbon electrode, Sensors Actuators B Chem. 126 (2007) 527–535.
[24] M.B. González, O.V. Quinzani, M.E. Vela, A. a. Rubert, G. Benítez, S.B. Saidman, Study of the electrosynthesis of hollow rectangular microtubes of polypyrrole, Synth. Met. 162 (2012) 1133–1139.
[25] G. Maduraiveeran, R. Ramaraj, A facile electrochemical sensor designed from gold nanoparticles embedded in three-dimensional sol-gel network for concurrent detection of toxic chemicals, Electrochem. Commun. 9 (2007) 2051–2055.
[26] J. Li, H. Xie, L. Chen, A sensitive hydrazine electrochemical sensor based on electrodeposition of gold nanoparticles on choline film modified glassy carbon electrode, Sensors Actuators B Chem. 153 (2011) 239–245.
[27] W. Chen, C.M. Li, P. Chen, C. Sun, Electrosynthesis and characterization of polypyrrole/Au nanocomposite, Electrochim. Acta 52 (2007) 2845–2849.
[28] M. Abdul Aziz, A.-N. Kawde, Gold nanoparticle-modified graphite pencil electrode for the high-sensitivity detection of hydrazine, Talanta 115 (2013) 214–221.
[29] A. Hallik, A. Alumaa, J. Tamm, V. Sammelselg, M. Väärtn ou, A. Jänes, E. Lust, Analysis of electrochemical impedance of polypyrrole–sulfate and polypyrrole–perchlorate films, Synth. Met. 156 (2006) 488–494.
[30] J. Li, H. Xie, Y. Li, Fabrication of gold nanoparticles/polypyrrole composite-modified electrode for sensitive hydroxylamine sensor design, J. Solid State Electrochem. 16 (2011) 795–802.
[31] L. Wang, J. Bai, P. Huang, H. Wang, L. Zhang, Y. Zhao, Self-assembly of gold nanoparticles for the voltammetric sensing of epinephrine, Electrochem. Commun. 8 (2006) 1035–1040.
[32] A. Hermas, M. Nakayama, K. Ogura, Formation of stable passive film on stainless steel by electrochemical deposition of polypyrrole, Electrochim. Acta 50 (2005) 3640–3647.
[33] R. Ramaraj, G. Maduraiveeran, Nanostructured Materials for Electrochemical Biosensors, Nova Science Publishers, Inc., New York, 2009.
[34] G. Láng, M. Ujvári, T. Rokob, G. Inzelt, The brush model of the polymer films–analysis of the impedance spectra of Au,Pt–poly(o-phenylenediamine) electrodes, Electrochim. Acta 51 (2006) 1680–1694.
[35] G. Inzelt, G.G. Láng, S. Cosnier, A. Karyakin (Eds.), Electropolymerization: Concepts, Materials and Applications, Wiley-VCH Verlag Gmbh and Co, Weinheim, 2010, pp. 51–76 Ch.3.
[36] Y. Wang, E. Laborda, R.G. Compton, Electrochemical oxidation of nitrite: kinetic, mechanistic and analytical study by square wave voltammetry, J. Electroanal. Chem. 670 (2012) 56–61.
[37] A.J. Bard, L.R. Faulkner, Electrochemical Methods, J. Wiley and Sons, New York, 1980.
[38] A.D. Goolsby, D.T. Sawyer, The electrochemical oxidation of hydroxylamine at platinum and gold electrodes in dimethylsulfoxlde, J. Electroanal. Chem. 19 (1968) 405–411.
[39] L. Shi, T. Wu, P. He, D. Li, C. Sun, J. Li, Amperometric sensor for hydroxylamine based on hybrid nickel-cobalt hexacyanoferrate modified electrode, Electroanalysis 17 (2005) 2190–2194.
[40] X. Cui, L. Hong, X. Lin, Electrocatalytic oxidation of hydroxylamine on glassy carbon electrodes modified by hybrid copper-cobalt hexacyano- ferrate films, Anal. Sci. 18 (2002) 543–547.
[41] K. Zhao, H. Song, S. Zhuang, L. Dai, P. He, Y. Fang, Determination of nitrite with the electrocatalytic property to the oxidation of nitrite on thionine modified aligned carbon nanotubes, Electrochem. Commun. 9 (2007) 65–70.
[42] M. Parsaeia, Z. Asadia, S. Khodadoust, A sensitive electrochemical sensor for rapid and selective determination of nitrite ion in water samples using modified carbon paste electrode with a newly synthesized cobalt(II)-Schiff base complex and magnetite nanospheres, Sensors Actuators B Chem. 220 (2015) 1131–11385.
[43] M. Bertotti, D. Pletcher, A study of nitrite oxidation at platinum microelectrodes, J. Braz. Chem. Soc. 8 (1997) 391–395.